The enhancement of local air pollution by urban CO_2 domes

Mark Z. Jacobson

Department of Civil and Environmental Engineering, Stanford University, Stanford, California 94305-4020, USA; Email: jacobson@stanford.edu; Tel: (650) 723-6836

October 3, 2009

Abstract

Data suggest that domes of high CO_2 levels form over cities. Despite our knowledge of these domes for over a decade, no study has contemplated their effects on local temperature or water vapor or the resulting feedback to air pollution and health. In fact, all air pollution regulations worldwide assume arbitrarily that such domes have no local health impact and carbon policy proposals, such as "cap and trade" implicitly assume that CO_2 impacts are the same regardless of where emissions occur. Here, it is found through data-evaluated numerical modeling with telescoping domains from the globe to the U.S., California, and Los Angeles, that local CO_2 emissions in isolation may increase local ozone and particulate matter, thus mortality by on the order of 50-100 deaths/yr in California and 300-1000 deaths/yr in the U.S. As such, reducing locally-emitted CO_2 will reduce local air pollution mortality even if CO_2 in adjacent regions is not controlled. This result contradicts the basis for air pollution regulations worldwide, none of which considers controlling local CO_2 based on its local health impacts. It also suggests that implementation of a "cap and trade" policy should consider the location of CO_2 emissions, as the underlying assumption of the policy is incorrect.

Introduction

Although CO_2 is generally well-mixed in the atmosphere, data indicate that its mixing ratios are higher in urban than in background air, resulting in *urban CO_2 domes* (1-5). Measurements in Phoenix, for example, indicate that peak and mean CO_2 in the city center are 75% and 38-43% higher, respectively, than in surrounding rural areas (2). Many recent studies have examined the impact of global greenhouse gases on air pollution (6-14). However, no study has isolated the impact of locally-emitted CO_2 on local air pollution, health, or climate. One reason is that model simulations of such an effect require treatment of meteorological feedbacks to gas, aerosol, and cloud changes, and few models include such feedbacks in deatil. Second, local CO_2 emissions are close to the ground, where the temperature contrast between the Earth's surface and the lowest CO_2 layers is small. However, studies have not considered that CO_2 domes result in CO_2 gradients up to high altitude. If locally-emitted CO_2 increases local air pollution, then cities, counties, states, and small countries can reduce air pollution health problems by reducing their own CO_2 emissions, regardless of whether other air pollutants are reduced locally or whether other locations reduce CO_2.

Methodology and Evaluation

For this study, the nested global-through-urban 3-D model, GATOR-GCMOM (14-19) was use to examine the effects of locally-emitted CO_2 on local climate and air pollution. A nested model is one that telescopes from a large scale to more finely-resolved domains. The model and its feedbacks are described in the Supplemental Information. Example CO_2 feedbacks treated include those to heating rates, thus temperatures, which affected (a) local temperature and pressure gradients, stability, wind speeds, and gas/particle transport, (b) water evaporation rates, (c) the relative humidity and particle swelling, and (d) temperature-dependent natural emissions, air chemistry, and particle microphysics. Changes in CO_2 also affected (e) photosynthesis and respiration rates, (f) dissolution and evaporation rates of CO_2 into the ocean, (g) weathering rates, (h) ocean pH and chemical composition, (i) sea

spray pH and composition, (j) and rainwater pH and composition. Changes in sea spray composition, in turn, affected sea spray radiative properties, thus heating rates.

The model was nested from the globe (resolution 4º SN x 5º WE) to the U.S. (0.5º x0.75º), California (0.20ºx0.15º), and Los Angeles (0.45ºx0.05º). The global domain included 47 sigma-pressure layers up to 0.22 hPa (≈60 km), with high resolution (15 layers) in the bottom 1 km. The nested regional domains included 35 layers exactly matching the global layers up to 65 hPa (≈18 km). The model was initialized with 1-degree global reanalysis data (20) but run without data assimilation or model spinup.

Three original pairs of baseline and sensitivity simulations were run: one pair nested from the globe to California for one year, one pair nested from the globe to California to Los Angeles, for two sets of three months (Feb-Apr, Aug-Oct), and one pair nested from the globe to the U.S. for two sets of three months (Jan-Mar, Jul-Sep). A second 1-year simulation pair was run for California for a different year as well. In each sensitivity simulation, only anthropogenic CO_2 emissions ($emCO_2$) were removed from the finest domain. Initial ambient CO_2 was the same in all domains of both simulations and $emCO_2$ was the same in the parent domains of both. As such, all resulting differences were due solely to locally-emitted (in the finest domain) CO_2.

The model and comparisons with data have been described in over 50 papers, including recently (14-19). Figure 1 further compares modeled O_3, PM_{10}, and CH_3CHO from August 1-7 of the baseline (with $emCO_2$) and sensitivity (no $emCO_2$) simulations from the Los Angeles domain with data. The comparisons indicate very good agreement with respect to ozone in particular. Since $emCO_2$ was the only variable that differed between the simulations, it was the causal factor in the day and night increase in O_3, PM_{10}, and CH_3CHO seen in Fig. 1.

Results

Figure 2a shows the modeled contribution of California's CO_2 emissions to column CO_2, averaged over a year. The CO_2 domes over Los Angeles, the San Francisco Bay Area, and much of the Central Valley are evident. The largest surface CO_2 increase (5%, or 17.5 ppmv) was lower than observed

increases in cities (2) since the resolution of the California domain was coarser than the resolution of measurements. As shown for Los Angeles shortly, an increase in model resolution increases the magnitude of the surface and column CO_2 dome.

Population-weighted (PW) and domain-averaged (DA) changes in several parameters can help to elucidate the effects of the CO_2 domes. A PW value is the product of a parameter value and population in a grid cell, summed over all grid cells, all divided by the summed population among all cells. Thus, a PW value indicates changes primarily in populated areas whereas a DA value indicates changes everywhere, independent of population. The PW and DA increases in surface CO_2 due to emCO_2 were 7.4 ppmv and 1.3 ppmv, respectively, but the corresponding increases in column CO_2 were 6.0 g/m^2 and 1.53 g/m^2, respectively, indicating that changes in column CO_2 were spread horizontally more than were changes in surface CO_2. This is because local emCO_2 starts mixing vertically into the convective mixed layer during the day and residual layer and above at night, where horizontal winds are faster than at the surface. The surface losses are quickly replaced with more local CO_2 emissions.

The CO_2 increases in California increased the PW air temperature by about 0.0063 K, more than it changed the domain-averaged air temperature (+0.00046) (Fig. 2b). Thus, CO_2 domes had greater temperature impacts where the CO_2 was emitted and where people lived than they had in the domain average. This result held for the effects of emCO_2 on column water vapor (Fig. 2c - PW: +4.3 g/m^2; DA: +0.88 g/m^2), ozone (Fig. 2d – PW: +0.06 ppbv; DA: +0.0043 ppbv), $PM_{2.5}$ (Fig. 2f – PW: +0.08 μg/m^3; DA: -0.0052 μg/m^3), PAN (Fig. 2h – PW: +0.002 ppbv; DA: -0.000005 ppbv) and particle nitrate (Fig. 2i – PW: +0.030 μg/m^3; DA: +0.00084 μg/m^3).

Figure 3 elucidates spatial correlations between changes in local ambient CO_2 caused by emCO_2 and changes in other parameters. Increases in temperature, water vapor, and ozone correlated positively and with statistical significance (p«0.05) with increases in CO_2. Ozone increases also correlated positively and with strong significance with increases in water vapor and temperature. A previous study found that increases in temperature and water vapor both increase ozone at high ozone but cause little change in ozone at low ozone (14), consistent with this result.

$PM_{2.5}$ correlated slightly negatively (r=0.017) but without statistical significance, with higher temperature and much more positively (r=0.23) and with strong significance (p<0.0001) with higher water vapor in California. Higher temperature decreased $PM_{2.5}$ by increasing vapor pressures thus PM evaporation and by enhancing precipitation in some locations. Some $PM_{2.5}$ decreases with higher temperature were offset by biogenic organic emission increases with higher temperatures followed by biogenic oxidation to organic PM. But, in populated areas of California, biogenic emissions are relatively low. Some $PM_{2.5}$ decreases were also offset by slower winds caused by enhanced boundary-layer stability from CO_2. While higher temperature slightly decreased $PM_{2.5}$, higher water vapor due to emCO_2 increased $PM_{2.5}$ by increasing aerosol water content, increasing nitric acid and ammonia gas dissolution, forming more particle nitrate (Fig. 2i) and ammonium. Higher ozone from higher water vapor also increased oxidation of organic gases to organic PM. Overall, $PM_{2.5}$ increased with increasing CO_2, but because of the opposing effects of temperature and water vapor on $PM_{2.5}$, the net positive correlation was weak (r=0.022) and not statistically significant (p=0.17). However, when all CO_2 increases below 1 ppmv were removed, the correlation improved substantially (r=0.047, p=0.07). Further, the correlation was strongly statistically significant for Los Angeles and U.S. domains, as discussed shortly.

Health effect rates (y) due to pollutants in each model domain were determined from

$$y = y_0 \sum_i \left\{ P_i \sum_t \left(1 - \exp\left[-\beta \times \max\left(x_{i,t} - x_{th}, 0 \right) \right] \right) \right\} \quad (1)$$

where $x_{i,t}$ is the concentration in grid cell i at time t, x_{th} is the threshold concentration below which no health effect occurs, β is the fractional increase in risk per unit x, y_0 is the baseline health effect rate, and P_i is the grid cell population. Table 1 provides sums or values of P , β, y_0, and x_{th}. California's local CO_2 resulted in ~13 (with a range of 6-19 due to uncertainty in epidemiological data) additional ozone-related deaths/year (Fig. 2e), or 0.3% above the baseline 4600 (2300-6900) deaths/year (Table 1). Higher $PM_{2.5}$ due to emCO_2 contributed another ~39 (13-60) deaths/year (Fig. 2g), 0.2% above

the baseline death rate of 22,500 (5900-42,000) deaths/year. Changes in cancer due to emCO_2 were relatively small (Table 1). A second pair of simulations was run for California, starting one year after the first. The results of this simulation were similar to those for the first approximately the same number of overall deaths attributable to emCO_2.

Simulations for Los Angeles echo results for California but allowed for a more resolved picture of the effects of emCO_2. Figure 4 (Feb-Apr) indicates that the near-surface CO_2 dome that formed over Los Angeles peaked at about 34 ppmv, twice that over the coarser California domain. The column difference indicates a spreading of the dome over a larger area than the surface dome. In Feb-Apr and Aug-Oct, emCO_2 enhanced PW ozone and $PM_{2.5}$, increasing mortality (Fig. 4, Table 1) and other health effects (Table 1). The causes of such increases, however, differed with season. From Feb-Apr, emCO_2 increased surface temperatures and water vapor over the Los Angeles basin (Fig. 4). This slightly enhanced ozone and $PM_{2.5}$, but the increase in the land-ocean temperature gradient by about 0.2 K over 50 km also increased sea-breeze wind speeds by ~0.06 m/s averaged over the month, increasing resuspension of road and soil dust and moving PM more to the eastern basin. From Aug-Oct, emCO_2 increased temperatures aloft, increasing the land-sea temperature gradient and wind speed aloft, increasing the flow of moisture from the ocean to land aloft, increasing water vapor transport, thereby increasing cloud optical depth by up to 0.4-0.6 over land, decreasing surface solar radiation by up to 3-4 W/m^2, and causing a net decrease in local ground temperatures by up to 0.2 K (Fig. 4). The excess water vapor aloft over land mixed to the surface (Fig. 4), increasing ozone (which increases chemically with water vapor at high ozone) and the relative humidity, which increased aerosol particle swelling, increasing gas growth onto aerosols, and reducing particle evaporation. In summary, emCO_2 increased ozone and $PM_{2.5}$ and their corresponding health effects in both seasons, increasing air pollution deaths in California and Los Angeles by about 50-100 per year (Fig. 4, Table 1). The positive spatial correlations between higher CO_2 and higher O_3 and $PM_{2.5}$ deaths were strongly significant (p<0.0001) (Fig. 4).

Figure 5 shows that, for the U.S. as a whole, the correlations between higher CO_2 and higher O_3 and $PM_{2.5}$ deaths were also both visually and statistically significant. The annual death rates due

to emCO_2 in the U.S. were ~770 (300-1000), with ~20% due to ozone. This death rate represented an enhancement of ~0.4% of the baseline death rate due to air pollution. With a U.S. anthropogenic emission rate of 5.76 GT-CO_2/yr (Table S2), this corresponds to ~134 (52-174) deaths/GT-CO_2/yr over the U.S. Death rates in Los Angeles for the Los Angeles simulation were higher than those for Los Angeles in the California or U.S. simulation due to the higher resolution of the Los Angeles simulations; thus, results for California and the U.S. may be conservative.

Implications

Worldwide, emissions of NO_x, HCs, CO, and PM are regulated. The few CO_2 regulations proposed to date have been justified based on its large-scale feedback to temperatures, sea levels, water supply, and global air pollution. No proposed CO_2 regulation is based on the potential impact of locally-emitted CO_2 on local pollution as such effects have been assumed not to exist (21). The result here suggests that reducing local CO_2 may reduce 300-1000 air pollution deaths/yr in the U.S. and 50-100/yr in California, even if CO_2 in adjacent regions is not controlled. The results, combined with those in (14), suggest that local CO_2 emissions should, in general, increase local ozone and particles due to feedbacks to temperatures, atmospheric stability, water vapor, humidity, winds, and precipitation. Thus, CO_2 emission controls are justified on the same grounds that NO_x, HC, CO, and PM emission regulations are justified. Results further imply that the assumption behind the "cap and trade" policy, namely that CO_2 emitted in one location has the same impact as CO_2 emitted in another, is incorrect, as CO_2 emissions in populated cities have larger health impacts than CO_2 emissions in unpopulated areas. As such, CO_2 cap and trade, if done, should consider the location of emissions to avoid additional health damage.

Acknowledgements

Support came from the U.S. Environmental Protection Agency grant RD-83337101-O, NASA grant NX07AN25G, and the NASA High-End Computing Program.

References

1. Idso, C.D., Idso, S.B. & Balling Jr. R.C. The urban CO_2 dome of Phoenix, Arizona. *Physical Geography* **19**, 95-108 (1998).

2. Idso, C.D., Idso, S.B. & Balling Jr., R.C. An intensive two-week study of an urban CO2 dome in Phoenix, Arizona, USA. *Atmos. Environ.* **35**, 995-1000 (2001).

3. Gratani, L. & Varone, L. Daily and seasonal variation of CO_2 in the city of Rome in relationship with the traffic volume. *Atmos. Environ.* **39**, 2619-2624 (2005).

4. Newman, S., Xu, X., Affek, H.P., Stolper, E., & Epstein, S. Changes in mixing ratio and isotopic composition of CO2 in urban air from the Los Angeles basin, California, between 1972 and 2003. *J. Geophys. Res.* **113**, D23304, doi:10.1029/2008JD009999 (2008).

5. Rigby, M., Toumi, R., Fisher, R. Lowry, D. & Nisbet, E.G. First continuous measurements of CO_2 mixing ratio in central London using a compact diffusion probe. *Atmos. Environ.* **42**, 8943-8953 (2008).

6. Knowlton, K., Rosenthal, J.E., Hogrefe, C., Lynn, B., Gaffin, S., Goldberg, R., Rosenzweig, C., Civerolo, K., Ku, J.-Y. & Kinney P.L. Assessing ozone-related health impacts under a changing climate. *Environ. Health Perspectives* **112**, 1557-1563 (2004).

7. Mickley, L.J., Jacob, D.J., Field, B.D. & Rind, D. Effects of future climate change on regional air pollution episodes in the United States. *Geophys. Res. Lett.* **31**, L24103, doi:10.1029/2004GL021216 (2004).

8. Stevenson, D., Doherty, R., Sanderson, M., Johnson, C., Collins, B. & Derwent, D. Impacts of climate change and variability on tropospheric ozone and its precursors. *Faraday Disc.* **130**, 1-17 (2005).

9. Brasseur, G.P., Schultz, M.M., Granier, C., Saunois, M., Diehl, T., Botzet, M. & Roeckner E. Impact of climate change on the future chemical composition of the global troposphere. *J. Clim.* **19**, 3932-3951 (2006).

10. Steiner, A.L., Tonse, S., Cohen, R.C., Goldstein, A.H. & Harley R.A. Influence of future climate and emissions on regional air quality in California. *J. Geophys. Res.* **111**, D18303, doi:10.1029/2005JD006935 (2006).

11. Unger, N., Shindell, D.T., Koch, D.M., Ammann, M., Cofala, J. & Streets D.G. Influences of man-made emissions and climate changes on tropospheric ozone, methane, and sulfate at 2030 from a broad range of possible futures. *J. Geophys. Res.* **111**, D12313, doi:10.1029/2005JD006518 (2006).

12. Liao, H., Chen, W.-T. & Seinfeld J.H. Role of climate change in global predictions of future tropospheric ozone and aerosols. *J. Geophys. Res.* **111**, D12304, doi:10.1029/2005JD006852 (2006).

13. Bell, M.L., Goldberg, R., Hogrefe, C., Kinney, P.L., Knowlton, K., Lynn, B., Rosenthal J., Rosenzweig, C. & Patz, J.A. Climate change, ambient ozone, and health in 50 U.S. cities. *Climatic Change* **82**, 61-76 (2007).

14. Jacobson, M.Z. On the causal link between carbon dioxide and air pollution mortality. *Geophys. Res. Lett.* **35**, L03809, doi:10.1029/2007GL031101 (2008).

15. Jacobson, M.Z. & Streets D.G. The influence of future anthropogenic emissions on climate, natural emissions, and air quality. *J. Geophys. Res.*, in press (2009).

16. Jacobson, M.Z. GATOR-GCMM: 2. A study of day- and nighttime ozone layers aloft, ozone in national parks, and weather during the SARMAP Field Campaign. *J. Geophys. Res.* **106**, 5403-5420 (2001).

17. Jacobson, M.Z., Kaufmann, Y.J. & Rudich, Y. Examining feedbacks of aerosols to urban climate with a model that treats 3-D clouds with aerosol inclusions. *J. Geophys. Res.* **112**, doi:10.1029/2007JD008922 (2007).

18. Jacobson, M.Z. Effects of wind-powered hydrogen fuel cell vehicles on stratospheric ozone and global climate. *Geophys. Res. Lett.* **35**, L19803, doi:10.1029/2008GL035102 (2008).

19. Jacobson, M.Z. The short-term effects of agriculture on air pollution and climate in California. *J. Geophys. Res.* **113**, D23101, doi:10.1029/2008JD010689 (2008).

20. Global Forecast System (GFS) (2007), 1° x 1° reanalysis fields, http://nomads.ncdc.noaa.gov/data/gfs-avn-hi/.

21. Johnson, S.L California State Motor Vehicle Pollution Control Standards; Notice of Decision Denying a Waiver of Clean Air Act Preemption for California's 2009 and Subsequent Model Year Greenhouse Gas Emission Standards for New Motor Vehicles. *Federal Register* **73** (45), 12,156-12,169 (2008).

22. United States Environmental Protection Agency (USEPA), AIR Data, http://www.epa.gov/air/data/ (2006).

23. Thurston, G.D. & Ito K. Epidemiological studies of acute ozone exposures and mortality. *J. Exposure Analysis and Env. Epidemiology* **11**, 286-294 (2001).

24. Hoyert, D.L., Heron, M.P., Murphy, S.L. & Kung H.-C. National Vital Statistics Reports, Vol. 54, No. 13, http://www.cdc.gov/nchs/fastats/deaths.htm (2006).

25. Merrill, C.T. & Elixhauser, A. HCUP Fact Book No. 6: Hospitalization in the United States, 2002. Appendix, www.ahrq.gov/data/hcup/factbk6/factbk6e.htm (2005).

26. Mannino, D.M., Homa, D.M., Akinbami, L.J., Moorman, J.E., Gwynn, C. & Redd S.C. Center for Disease Control Morbidity and Mortality Weekly Report. *Surveillance Summaries* **51** (SS01), 1-13 (2002).

27. Ostro, B.D., Tran, H. & Levy, J.I. The health benefits of reduced tropospheric ozone in California. *J. Air & Waste Manage. Assoc.* **56**, 1007-1021 (2006).

28. Pope III, C.A., Burnett, R.T., Thun, M.J., Calle, E.E., Krewski, D., Ito, K., Thurston, G.D. Lung cancer, cardiopulmonary mortality, and long-term exposure to fine particulate air pollution. *JAMA,* **287**, 1132-1141 (2002).

Figure Captions

Figure 1. Paired-in-time-and-space comparisons of modeled baseline (solid lines), modeled no-emCO_2 (dashed lines), and data (22) (dots) for ozone, sub-10-μm particle mass, and acetaldehyde from the Los Angeles domain for August 1-7, 2006.

Figure 2. Modeled annually averaged difference for several surface or column parameters in California, parts of Nevada, and parts of New Mexico when two simulations (with and without emCO_2) were run. The numbers in parentheses are population-weighted changes.

Figure 3. Scatter plots of paired-in-space one-year-averaged changes between several parameter pairs, obtained from all near-surface grid cells of the California domain. Also shown is an equation for the linear fit through the data points in each case and the *r* and *p* values for the fits.

Figure 4. Same as Fig. 2., but for the Los Angeles domain and for Feb-Apr and Aug-Oct. Also shown are scatter plots for Aug-Oct similar to those for Fig. 3.

Figure 5. Same as Fig. 2., but for the U.S. domain and for Jun-Aug. Also shown are scatter plots similar to those for Fig. 3.

Table 1. Summary of locally-emitted CO_2's ($emCO_2$) effects on cancer, ozone mortality, ozone hospitalization, ozone emergency-room (ER) visits, and particulate-matter mortality in California (CA), Los Angeles (LA), and the United States (US). Results are shown for the with-$emCO_2$ emissions simulation ("Base") and the difference between the base and no $emCO_2$ emissions simulations ("Base minus no-$emCO_2$") for each case. The domain summed populations in the CA, LA, and US domains were 35.35 million, 17.268 million, and 324.07 million, respectively. All concentrations except the second $PM_{2.5}$, which is an all-land average, are near-surface values weighted spatially by population. CA results were for an entire year, LA results were an average of Feb-Apr and Aug-Oct, and US results were an average of Jan-Mar and Jul-Sep.

	Annual base CA	Base minus no $emCO_2$ CA	Annual Base LA	Base minus no $emCO_2$ LA	Annual Base US	Base minus no $emCO_2$ US
Ozone ≥ 35 ppbv (ppbv)	47.4	+0.060	44.7	+0.12	47.0	+0.044
$PM_{2.5}$ (μg/m^3) (pop-weight)	50.0	+0.08	36	+0.29	64.4	+0.041
$PM_{2.5}$ (μg/m^3) (all land)	21.5	-0.007	25.8	+0.06	32.8	+0.039
Formaldehyde (ppbv)	4.43	+0.0030	4.1	+0.054	6.75	+0.066
Acetaldehyde (ppbv)	1.35	+0.0017	1.3	+0.021	2.45	+0.016
1,3-Butadiene (ppbv)	0.11	-0.00024	0.23	+0.0020	0.077	+0.0005
Benzene (ppbv)	0.30	-0.00009	0.37	+0.0041	0.34	+0.020
Cancer						
USEPA cancers/yr$^+$	44.1	0.016	22.0	+0.28	573	+6.9
OEHHA cancers/yr$^+$	54.4	-0.038	37.8	+0.39	561	+11.8
Ozone health effects						
High O_3 deaths/yr*	6860	+19	2140	+20	52,300	+245
Med. O_3 deaths/yr*	4600	+13	1430	+14	35,100	+166
Low O_3 deaths/yr*	2300	+6	718	+7	17,620	+85
O_3 hospitalizations/yr*	26,300	+65	8270	+75	200,000	+867
Ozone ER visits/yr*	23,200	+56	7320	+66	175,000	+721
PM health effects						
High $PM_{2.5}$ deaths/yr^	42,000	+60	16,220	+147	44,800	+810
Medium $PM_{2.5}$ deaths/yr^	22,500	+39	8500	+81	169,000	+607
Low $PM_{2.5}$ deaths/yr^	5900	+13	2200	+22	316,000	+201

(+) USEPA and OEHHA cancers/yr were found by summing, over all model surface grid cells and the four carcinogens (formaldehyde, acetaldehyde, 1,3-butadiene, and benzene), the product of individual CUREs (cancer unit risk estimates=increased 70-year cancer risk per μg/m^3 sustained concentration change), the mass concentration (μg/m^3) (for baseline statistics) or mass concentration difference (for difference statistics) of the carcinogen, and the population in the cell, then dividing by the population of the model domain and by 70 yr. USEPA CURES are $1.3x10^{-5}$ (formaldehyde), $2.2x10^{-6}$ (acetaldehyde), $3.0x10^{-5}$ (butadiene), $5.0x10^{-6}$ (=average of $2.2x10^{-6}$ and $7.8x10^{-6}$) (benzene)

(www.epa.gov/IRIS/). OEHHA CUREs are $6.0x10^{-6}$ (formaldehyde), $2.7x10^{-6}$ (acetaldehyde), $1.7x10^{-4}$ (butadiene), $2.9x10^{-5}$ (benzene) (www.oehha.ca.gov/risk/ChemicalDB/index.asp).

(*) High, medium, and low deaths/yr, hospitalizations/yr, and emergency-room (ER) visits/yr due to short-term O_3 exposure were obtained from Equation 1, assuming a threshold of 35 ppbv (23). The baseline 2003 U.S. death rate (y_0) was 833 deaths/yr per 100,000 (24). The baseline 2002 hospitalization rate due to respiratory problems was 1189 per 100,000 (25). The baseline 1999 all-age emergency-room visit rate for asthma was 732 per 100,000 (26). The fractional increases (β) in the number of deaths from all causes due to ozone were 0.006, 0.004, and 0.002 per 10 ppbv increase in daily 1-hr maximum ozone (27). These were multiplied by 1.33 to convert the risk associated with a 10 ppbv increase in 1-hr maximum O_3 to that associated with a 10 ppbv increase in 8-hour average O_3 (23). The central value of the increased risk of hospitalization due to respiratory disease was 1.65% per 10 ppbv increase in 1-hour maximum O_3 (2.19% per 10 ppbv increase in 8-hour average O_3), and that for all-age ER visits for asthma was 2.4% per 10 ppbv increase in 1-hour O_3 (3.2% per 10 ppbv increase in 8-hour O_3) (25, 26).

(^) The death rate due to long-term $PM_{2.5}$ exposure was calculated from Equation 1. Increased death risks to those ≥30 years were 0.008 (high), 0.004 (medium), and 0.001 (low) per 1 $\mu g/m^3$ $PM_{2.5}$ >8 $\mu g/m^3$ based on 1979-1983 data (28). From 0-8 $\mu g/m^3$, the increased risks here were assumed =¼ those >8 $\mu g/m^3$ to account for reduced risk near zero $PM_{2.5}$ (14). The all-cause 2003 U.S. death rate of those ≥30 years was 809.7 deaths/yr per 100,000 total population.

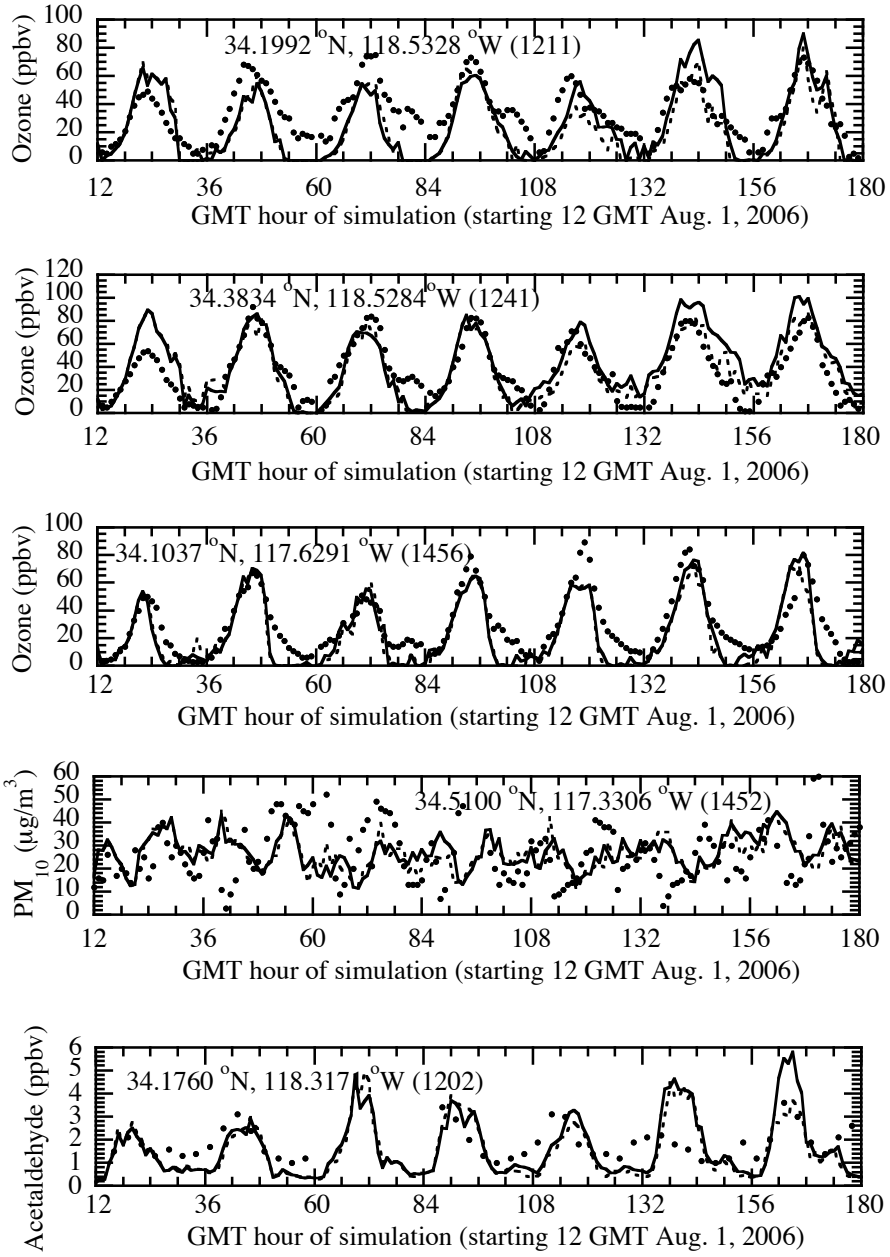
34.1992 °N, 118.5328 °W (1211)
Ozone (ppbv)
GMT hour of simulation (starting 12 GMT Aug. 1, 2006)
34.3834 °N, 118.5284 °W (1241)
Ozone (ppbv)
GMT hour of simulation (starting 12 GMT Aug. 1, 2006)
34.1037 °N, 117.6291 °W (1456)
Ozone (ppbv)
GMT hour of simulation (starting 12 GMT Aug. 1, 2006)
34.5100 °N, 117.3306 °W (1452)
PM10 (µg/m3)
GMT hour of simulation (starting 12 GMT Aug. 1, 2006)
34.1760 °N, 118.3171 °W (1202)
Acetaldehyde (ppbv)
GMT hour of simulation (starting 12 GMT Aug. 1, 2006)

Figure 1

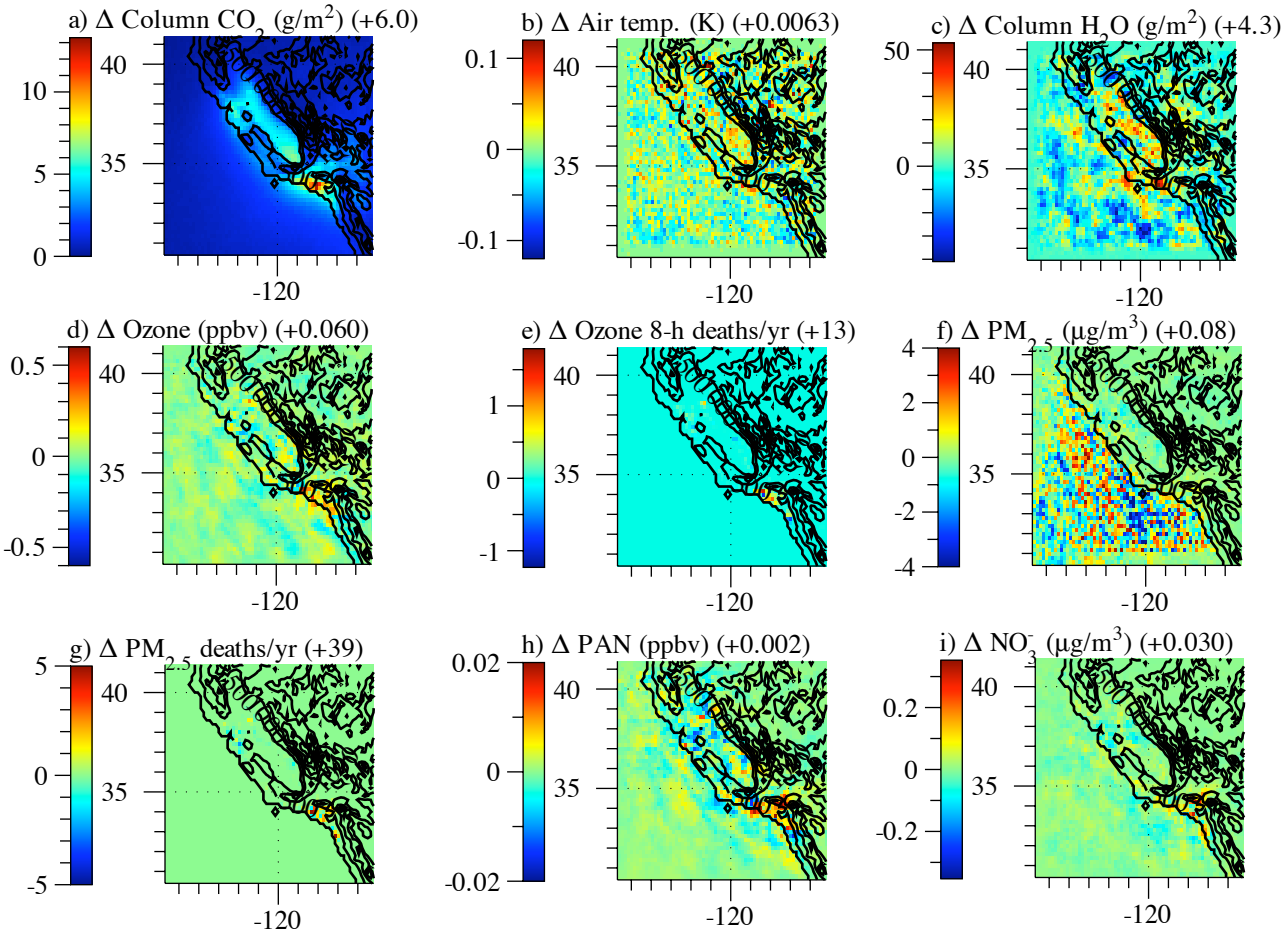
a) Δ Column CO_2 (g/m^2) (+6.0)
b) Δ Air temp. (K) (+0.0063)
c) Δ Column H_2O (g/m^2) (+4.3)
d) Δ Ozone (ppbv) (+0.060)
e) Δ Ozone 8-h deaths/yr (+13)
f) Δ $PM_{2.5}$ ($\mu g/m^3$) (+0.08)
g) Δ $PM_{2.5}$ deaths/yr (+39)
h) Δ PAN (ppbv) (+0.002)
i) Δ NO_3^- ($\mu g/m^3$) (+0.030)
40
35
-120

Figure 2

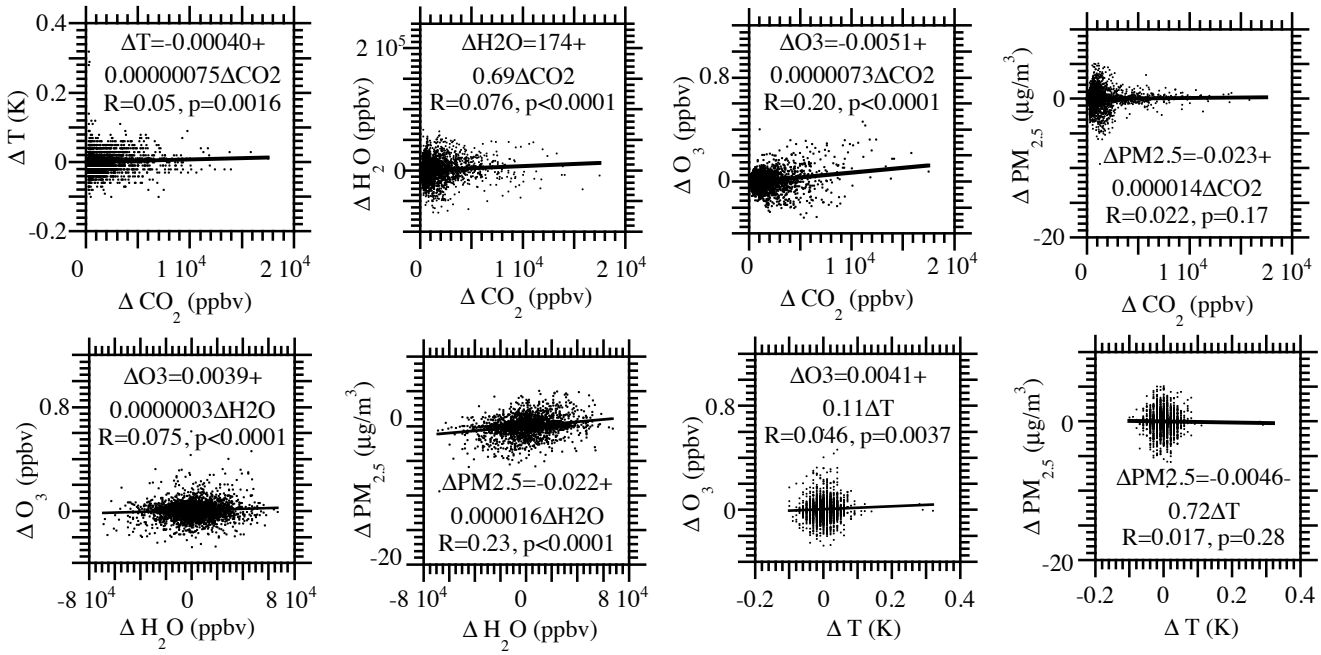
ΔT=-0.00040+
0.00000075ΔCO2
R=0.05, p=0.0016
Δ T (K)
Δ CO2 (ppbv)
ΔH2O=174+
0.69ΔCO2
R=0.076, p<0.0001
Δ H2O (ppbv)
Δ CO2 (ppbv)
ΔO3=-0.0051+
0.0000073ΔCO2
R=0.20, p<0.0001
Δ O3 (ppbv)
Δ CO2 (ppbv)
ΔPM2.5=-0.023+
0.000014ΔCO2
R=0.022, p=0.17
Δ PM2.5 (μg/m3)
Δ CO2 (ppbv)
ΔO3=0.0039+
0.0000003ΔH2O
R=0.075, p<0.0001
Δ O3 (ppbv)
Δ H2O (ppbv)
ΔPM2.5=-0.022+
0.000016ΔH2O
R=0.23, p<0.0001
Δ PM2.5 (μg/m3)
Δ H2O (ppbv)
ΔO3=0.0041+
0.11ΔT
R=0.046, p=0.0037
Δ O3 (ppbv)
Δ T (K)
ΔPM2.5=-0.0046-
0.72ΔT
R=0.017, p=0.28
Δ PM2.5 (μg/m3)
Δ T (K)

Figure 3

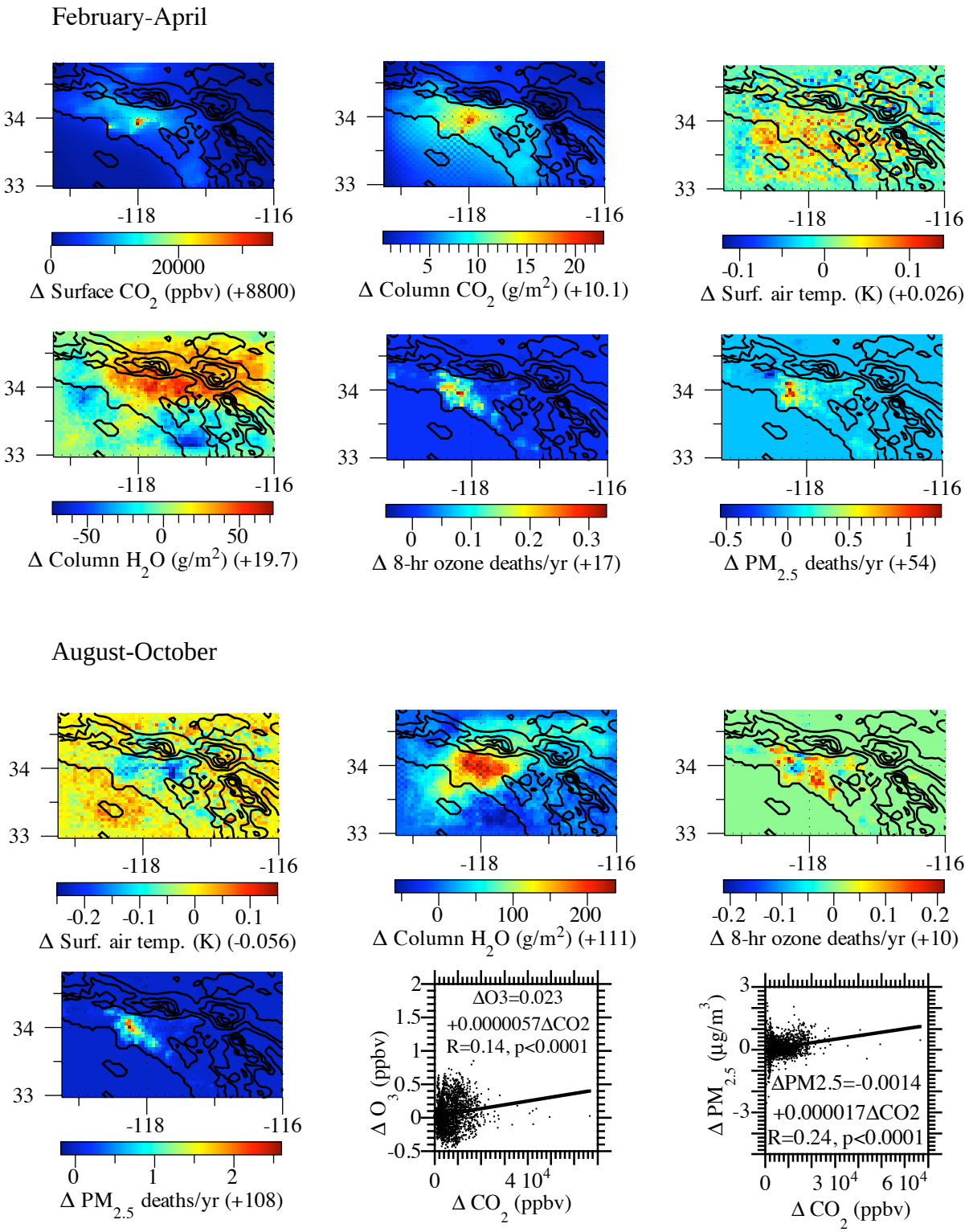
February-April
34
33
-118
-116
0
20000
Δ Surface CO2 (ppbv) (+8800)
5
10
15
20
Δ Column CO2 (g/m2) (+10.1)
-0.1
0
0.1
Δ Surf. air temp. (K) (+0.026)
-50
0
50
Δ Column H2O (g/m2) (+19.7)
0
0.1
0.2
0.3
Δ 8-hr ozone deaths/yr (+17)
-0.5
0
0.5
1
Δ PM2.5 deaths/yr (+54)
August-October
-0.2
-0.1
0
0.1
Δ Surf. air temp. (K) (-0.056)
0
100
200
Δ Column H2O (g/m2) (+111)
-0.2
-0.1
0
0.1
0.2
Δ 8-hr ozone deaths/yr (+10)
0
1
2
Δ PM2.5 deaths/yr (+108)
ΔO3=0.023
+0.0000057ΔCO2
R=0.14, p<0.0001
Δ O3 (ppbv)
4 10^4
Δ CO2 (ppbv)
ΔPM2.5=-0.0014
+0.000017ΔCO2
R=0.24, p<0.0001
Δ PM2.5 (μg/m3)
3 10^4
6 10^4
Δ CO2 (ppbv)

Figure 4

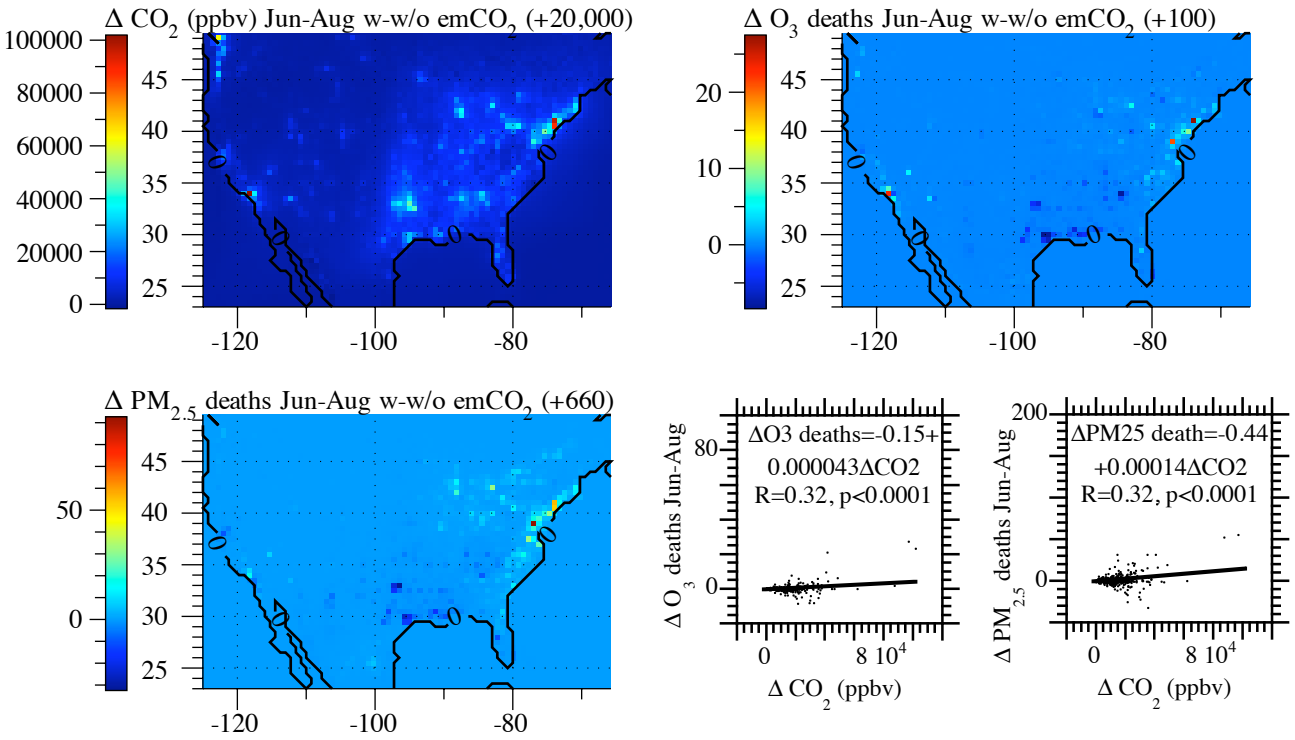
Δ CO2 (ppbv) Jun-Aug w-w/o emCO2 (+20,000)
Δ O3 deaths Jun-Aug w-w/o emCO2 (+100)
Δ PM2.5 deaths Jun-Aug w-w/o emCO2 (+660)
ΔO3 deaths=-0.15+
0.000043ΔCO2
R=0.32, p<0.0001
ΔPM25 death=-0.44
+0.00014ΔCO2
R=0.32, p<0.0001
Δ O3 deaths Jun-Aug
Δ PM2.5 deaths Jun-Aug
Δ CO2 (ppbv)

Figure 5